Propagating modes in a periodic wave guide in the semi-classical limit

2002 J. Phys. A: Math. Gen. 35 1339

(http://iopscience.iop.org/0305-4470/35/6/302)

INSTITUTE OF PHYSICS PUBLISHING JOURNAL OF PHYSICS A: MATHEMATICAL AND GENERAL

J. Phys. A: Math. Gen. **35** (2002) 1339–1356 PII: S0305-4470(02)25096-9

Propagating modes in a periodic wave guide in the semi-classical limit

Frédéric Faure[1]

LPMMC (Maison des Magisteres Jean Perrin, CNRS), BP 166, 38042 Grenoble Cedex 9, France

E-mail: frederic.faure@ujf-grenoble.fr

Received 22 May 2001, in final form 7 November 2001
Published 1 February 2002
Online at stacks.iop.org/JPhysA/35/1339

Abstract

It is well known that the number of propagating modes in a uniform wave guide is the transverse section divided by the wavelength λ (for a two-dimensional (2D) wave guide). In this paper we study the number of propagating modes N_{modes} in the limit of small λ, in the case where the section is non-constant but periodic. Using results of a study done by Asch and Knauf (Asch J and Knauf A 1998 *Nonlinearity* **11** 175–200), we show that for small λ, N_{modes} grows like μ_b/λ where μ_b is the measure of the ballistic classical trajectories inside the guide. In the case of an ergodic wave guide, where there are no ballistic trajectories but only diffusive trajectories, we show that N_{modes} grows like $\sqrt{D}/\sqrt{\lambda}$ where D is the diffusion constant. These results are generalized for any Hamiltonian periodic in one direction, and numerical results with the kicked Harper model are given. N_{modes} can be related to the Landauer conductance.

PACS numbers: 42.25.Bs, 05.60.Cd, 05.60.Gg, 05.45.Mt, 05.45.Pq, 03.65.Sq

1. Introduction

There is an intense activity of research concerning waves in complex media where different approaches and tools are used but some common concepts emerge [3, 5]. Complex media mean a disordered potential or a chaotic one, i.e. generating strong mixing and interferences of waves like chaotic cavities. This activity concerns both classical waves in optics or acoustics, and quantum waves like electronic waves in mesoscopic devices, for example.

One of the possible approaches, called semi-classical analysis, consists of studying the problem in the limit where the wavelength λ is small compared to the typical scale of the potential. The behaviour of the waves can then be explained or interpreted in terms of the behaviour of classical particles submitted to the same potential. Classical dynamics takes

[1] http://lpm2c.polycnrs-gre.fr/faure.

place in Hamiltonian phase space and can exhibit a rich structure (with resonances, chaos, stability islands, ...) which has a non-trivial counterpart in wave behaviour [5]. Semi-classical analysis can give a good insight into the original problem of waves. However, the difficulty is to establish precise correspondences between the properties of classical dynamics and wave dynamics.

In this paper we address the problem of transport of waves in a structure which is periodic in one direction, with no disorder. Experimentally, this concerns optical waves in a guide [8], acoustic waves in water [12], or quantum electronic waves in mesoscopic structures. We focus on structures which are periodic in one dimension z, and which confine in the other directions. Due to the periodicity, one can define some propagating modes in the wave guide (Bloch waves) and the number of modes at a given energy $N_{\text{modes}}(E)$, which can be related to the Landauer conductance, is a physical quantity quite accessible experimentally. The behaviour of a classical particle in the same periodic guide can be variable depending on the initial conditions. Some trajectories can be ballistic and propagate like $z(t) \simeq vt$, and others can be diffusive and propagate like $\langle z^2(t)\rangle \simeq Dt$. Asch and Knauf [1] have shown the implications of the classical ballistic trajectories on the wave spectrum. We use their analysis and results here to obtain a precise expression of $N_{\text{modes}}(E)$ in terms of the measure of the ballistic trajectories in the guide μ_b, and show that $N_{\text{modes}}(E)$ behaves like μ_b/λ when the wavelength λ goes to zero in the semi-classical limit. As shown below, this result is obvious in the case of a uniform wave guide.

Some ergodic periodic structures, like the well-known periodic Sinaï billiard, can possess no ballistic trajectories at all (i.e. ballistic trajectories have zero measure $\mu_b = 0$), but N_{modes} is nevertheless non-zero. By a refinement of the previous semi-classical correspondence, we show that N_{modes} is proportional to $\sqrt{D}/\sqrt{\lambda}$, a sub-leading contribution coming from the diffusive trajectories, with diffusive constant D. This relation between the number of modes N_{modes} and the classical diffusive constant seems *a priori* paradoxical, because a propagating mode is ballistic, but is perhaps more clear in a dynamical point of view: if we launch a wave packet, it will diffuse up to the Heisenberg time, according to a classical distribution of points, but for time greater than t_{H}, the energy levels no longer have a collective effect, and the wave packet will spread ballistically. So t_{H} plays a major role in obtaining $N_{\text{modes}} \propto \sqrt{D}/\sqrt{\lambda}$. This has to be compared to the case of a wave packet in a disordered guide, where the wave packet diffuses up to the 'local Heisenberg time', also called the 'break-time', and localizes for longer times.

In the next section, starting from the Helmholtz equation for classical waves, we define the number of propagating modes $N_{\text{modes}}(E)$ from the band spectrum. Following the work of Asch and Knauf [1], we consider the quantum velocities $v_\hbar$ of the stationary states, and their distribution at a given energy $P_\hbar(v_\hbar, E)$. This distribution characterizes the quantum transport. $N_{\text{modes}}(E)$ is expressed with respect to $P_\hbar(v_\hbar, E)$ in equation (14).

In section 3, we consider the classical transport in the periodic guide: the distribution of classical velocities $P_t(v, E)$ is defined. We show how diffusive and ballistic properties of the classical transport can be extracted from it.

In section 4, we recall a result of Asch and Knauf [1] which gives a simple equivalence between $P_\hbar(v, E)$ and $\lim_{t\to\infty} P_t(v, E)$ (the classical asymptotic velocities distribution). From this, we deduce the leading term of $N_{\text{modes}}(E)$. In the case of an ergodic and diffusive guide, we state a more precise equivalence between $P_\hbar(v, E)$ and $P_{t_{\text{H}}}(v, E)$ where t_{H} is the Heisenberg time (note that $t_{\text{H}} \propto 1/\lambda \to \infty$ for $\lambda \to 0$). From this we obtain the sub-leading term of $N_{\text{modes}}(E)$.

In section 5, we show that the measure of classical ballistic trajectories μ_b can simply be measured on any Poincaré section, transverse to the periodic direction. This shows a strong

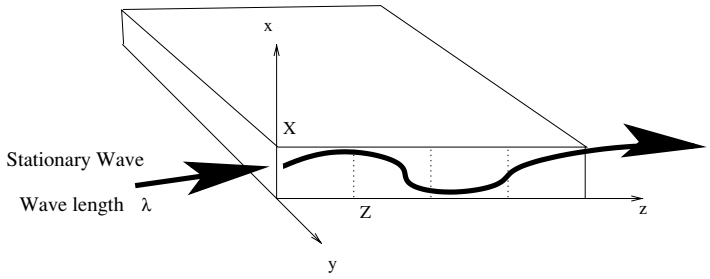

Figure 1. An optical z-periodic wave guide.

analogy of our result (26), with the standard Weyl formula counting the number of states, although $N_{\text{modes}}(E)$ cannot be estimated by the Weyl formula in a rigorous manner.

In section 6, we gives numerical results which confirm quite accurately all the previous relations. The model considered here is the well-known kicked Harper model. Then we conclude, giving possible refinements and perspectives of this work, and explain how the results are modified in any dimensions. We also discuss the applicability of our results in concrete physical systems where absorption and disorder effects occur.

2. Propagating modes and Floquet spectrum

2.1. Hamiltonian formulation for the stationary Helmholtz equation

To begin with a concrete example, let us consider the model of a planar (y, z) cavity, with constant width X in the x-direction (see figure 1). Inside the cavity, we assume an index $n(x, z)$ which does not depend on y. We assume perfect reflection on the two sides $x = 0$ and $x = X$. The Helmholtz equation for a scalar wave equation $\phi(x, y, z)$, assuming the form $\phi(x, y, z) = \phi(x, z) \exp(\mathrm{i}k_y y)$, is

$$\left(\partial_z^2 + \partial_x^2\right) \phi(x, z) + n^2(x, z)\frac{\omega^2}{c^2}\phi(x, z) = k_y^2 \phi(x, z) \tag{1}$$

with the Dirichlet boundary conditions,

$$\phi(0, z) = \phi(X, z) = 0 \qquad \forall z \tag{2}$$

where ω is the frequency of the wave, and c is the speed of the light.

We will assume that the internal index of the guide is periodic in the z-direction, with period Z:

$$n(x, z) = n(x, z + Z) \qquad \forall x, z.$$

In the following, we will define

$$\hbar = \frac{c}{\omega}$$

(which has nothing to do with the Planck constant, but is related to the wavelength of light in vacuum by $\lambda = 2\pi c/\omega = 2\pi\hbar = h$). This allows us to write equation (1) as a stationary Schrödinger equation

$$\hat{H}\phi = E\phi \tag{3}$$

with

$$\hat{H} = -\frac{\hbar^2}{2}\left(\partial_x^2 + \partial_z^2\right) + V(x, z) \qquad V(x, z) = -\tfrac{1}{2}n^2(x, z) \qquad E = \tfrac{1}{2}k_y^2\hbar^2. \tag{4}$$

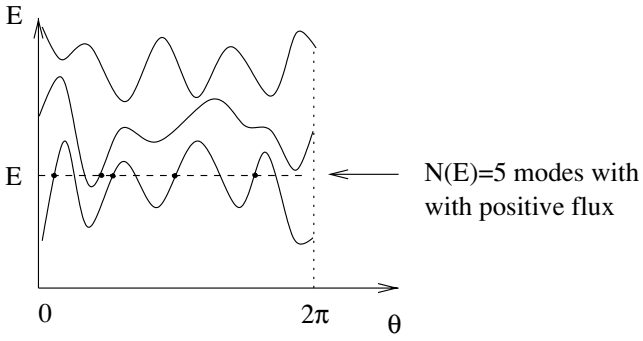

Figure 2. The propagating modes with positive flux are the intersections of the band spectrum with positive slope, with a fixed energy E.

Because the 'potential' $V(x, z)$ is Z-periodic in z, it is natural to consider the space of quasi-periodic functions as in Bloch theory,

$$\mathcal{H}_\theta = \{\phi(x, z) \text{ such that } \phi(x, z + Z) = T_{-Z}\phi = \mathrm{e}^{\mathrm{i}\theta}\phi(x, z)\} \tag{5}$$

which is the space of eigenvectors of the translation operator $T_{-Z} = \exp(\mathrm{i}Z(\mathrm{i}\partial_z))$ with eigenvalue $\exp(\mathrm{i}\theta)$. Because $[\hat{H}, T_Z] = 0$, $\hat{H}$ can be diagonalized in the space $\mathcal{H}_\theta$. Consider the energy surface in one cell (the set of points with the same energy E):

$$\Sigma_E = \{(x,\, p_x, z,\, p_z) \text{ such that } H(x,\, p_x, z,\, p_z) = E,\ 0 \leqslant z < Z\}. \tag{6}$$

Σ_E is a compact set, so the spectrum of $\hat{H}$ in the space $\mathcal{H}_\theta$ is discrete and can be written as

$$\hat{H}|\phi_n(\theta)\rangle = E_{n,\theta}|\phi_n(\theta)\rangle \qquad n \in \mathbb{N}. \tag{7}$$

(The total Hilbert space of functions $\mathcal{H}_{\text{tot}} = L^2(R_x \oplus R_y)$ is decomposed as $\mathcal{H}_{\text{tot}} = \int_\oplus \mathcal{H}_\theta \,\mathrm{d}\theta$.)

The spectrum of $\hat{H}$ is then a band spectrum for $\theta = 0 \to 2\pi$, sketched in figure 2. In this figure, the number of solutions of the Helmholtz equation (1) is equal to the number of intersections between the graph of energy band functions $E_n(\theta)$ and the line of constant energy $E = \frac{1}{2}k_y^2\hbar^2$.

The solutions of the Helmholtz equation (1) are the intersections of the bands with the fixed energy $E = \frac{1}{2}k_y^2\hbar^2$.

The slope of the band is related to the mean value of the velocity operator by the well-known Feynman–Hellmann relation,

$$\frac{\mathrm{d}E_{n,\theta}}{\mathrm{d}\theta} = \frac{\hbar}{Z}\langle\phi_n(\theta)|\hat{v}_z|\phi_n(\theta)\rangle \tag{8}$$

with

$$\hat{v}_z = \partial_{\hat{p}_z}\hat{H} = \hat{p}_z = -\mathrm{i}\hbar\frac{\partial}{\partial z}. \tag{9}$$

In the following, we will restrict our attention to positive propagating modes, i.e. states $|\phi_n(\theta)\rangle$ with a positive mean velocity, i.e. a positive slope $\mathrm{d}E_{n,\theta}/\,\mathrm{d}\theta$. The positive propagating modes are marked with a point in figure 2.

The number of these (positive) propagating modes at energy E can be written as

$$N_{\text{modes}}(E) = \#\left\{(n, \theta) \in \mathbb{N} \times [0, 2\pi[\text{ such that } E_{n,\theta} = E,\ \frac{\mathrm{d}E_{n,\theta}}{\mathrm{d}\theta} > 0\right\}. \tag{10}$$

The aim of this paper is to give the asymptotic behaviour of $N_{\text{modes}}(E)$ for $\hbar \to 0$.

Note that the Weyl formula which estimates the density of states in energy, would give the number of intersections of the bands with a vertical line in figure 2. So the Weyl formula cannot be used to estimate $N_{\text{modes}}(E)$. Nevertheless, in section 5 we will give a formula for $N_{\text{modes}}(E)$ very similar to the Weyl formula.

2.2. Example of a uniform guide

To help the reader, we recall here the simplest (and trivial) example of a wave guide with constant index $n(x, z) = n_0$. The stationary solutions of equation (3) are

$$\begin{aligned}
&\phi(x, z) = \mathrm{e}^{\mathrm{i}p_z z/\hbar} \sin(x p_x/\hbar).\\
&E = \tfrac{1}{2}\left(p_x^2 + p_z^2\right) - \tfrac{1}{2}n_0^2.\\
&p_x = k\pi\hbar/X \qquad k \in \mathbb{N}^*.\\
&p_z = \hbar(\theta + 2\pi l)/Z \qquad l \in \mathbb{Z}.
\end{aligned}$$

Because of the transverse quantization condition for p_x, there is a finite number of solutions given by (for $E = 0$)

$$N_{\text{modes}} = \left[\frac{2n_0 X}{h}\right] \tag{11}$$

where $[\cdot]$ is the integer part and $h = 2\pi\hbar$. This is a special case of our general result (equation (26)).

2.3. Distribution of quantal velocities

From figure 2, it is clear that the number of modes $N_{\text{modes}}(E)$, is closely related to the distribution of slopes $\mathrm{d}E_{n,\theta}/\mathrm{d}\theta$ of the bands at energy E. (A zero slope will give no intersection with a horizontal line, thus no mode.) We are now looking for such a relation. Asch and Knauf [1] define the distribution of quantum velocities as follows. From equation (8), for a given (n, θ), the quantum state $|\phi_n(\theta)\rangle$ of energy $E_{n,\theta}$ has a quantum velocity defined by

$$v_\hbar = \langle\phi_n(\theta)|\hat{v}_z|\phi_n(\theta)\rangle = \frac{Z}{\hbar}\frac{\mathrm{d}E_{n,\theta}}{\mathrm{d}\theta}. \tag{12}$$

The Weyl formula tells us that a quantum state occupies a volume h^2 in phase space. So it is natural to define the measure $P_\hbar(v_\hbar, E)\mathrm{d}v_\hbar\mathrm{d}E$ to be the image of the measure $(h^2\mathrm{d}n,\ \mathrm{d}\theta/(2\pi))$ by the application $(n, \theta) \to (v_\hbar, E_{n,\theta})$ (here $\mathrm{d}n$ denotes the punctual measure on $\mathbb{N}$). In other words, the definition of $P_\hbar$ is such that for any test function $F(v_\hbar, E)$,

$$\sum_n h^2 \int \frac{\mathrm{d}\theta}{2\pi} F(v_\hbar, E) = \iint F(v_\hbar, E)\, P_\hbar(v_\hbar, E)\, \mathrm{d}v_\hbar\, \mathrm{d}E. \tag{13}$$

This distribution of quantum velocities which is obtained from the Floquet spectrum has a classical counterpart, namely the distribution of classical velocities which will be defined in section 3.1. The equivalence of the two distributions will be discussed in section 4, and this equivalence will be the key point to obtain a semi-classical expression for the number of modes $N_{\text{modes}}(E)$, by using the following formula:

Property. *The number of modes at energy E is obtained by*

$$N_{\text{modes}}(E) = \frac{1}{hZ}\int_0^{+\infty} v_\hbar\, P_\hbar(v_\hbar, E)\, \mathrm{d}v_\hbar. \tag{14}$$

Proof. The definition equation (10) gives

$$N_{\text{modes}}(E) = \#\left\{(\theta, n) \in [0, 2\pi[\times\mathbb{N} \text{ such that } E_{n,\theta} = E,\ \frac{\mathrm{d}E_{n,\theta}}{\mathrm{d}\theta} > 0\right\}$$
$$= \sum_n \int \mathrm{d}\theta \delta(E - E_{n,\theta})\Theta\left(\frac{\mathrm{d}E_{n,\theta}}{\mathrm{d}\theta}\right)\frac{\mathrm{d}E_{n,\theta}}{\mathrm{d}\theta}.$$

From equations (12) and (13),

$$N_{\text{modes}}(E) = \frac{2\pi}{h^2}\iint \delta(E - E_{n,\theta})\Theta(v_\hbar)v_\hbar \frac{\hbar}{Z}P_\hbar \,\mathrm{d}v_\hbar \,\mathrm{d}E = \frac{1}{hZ}\int_0^{+\infty} v_\hbar P_\hbar(v_\hbar, E)\,\mathrm{d}v_\hbar. \qquad \square$$

Because of the fine band structure $N_{\text{modes}}(E)$ fluctuates with E at the scale of the mean level spacing ΔE. From the Weyl formula, $\Delta E \simeq h^2/\nu_E$, for $\hbar \to 0$ with $\nu_E = \int \delta(E - \mathcal{H}(\vec{x}, \vec{p}))\,\mathrm{d}\vec{x}\,\mathrm{d}\vec{p}$ the Liouville measure of the energy surface Σ_E. To eliminate these fluctuations, we consider the average value of $N_{\text{modes}}(E)$ over a finite (but small) interval of energy greater than ΔE,

$$\langle N_{\text{modes}}(E)\rangle \hat{=} \int N_{\text{modes}}(E')f(E' - E)\,\mathrm{d}E' \tag{15}$$

with f a smoothing function of compact support and $\int_{-\infty}^{+\infty} f(E) = 1$.

2.4. Formulation for a general Hamiltonian

We can easily generalize the preceding section, in order to embrace more general models in physics, such as motion in a general periodic potential, the motion of electrons in a periodic mesoscopic device with a magnetic field, or more abstract models, such as the (extensively studied) kicked Harper model, investigated in section 6, which has the advantage of being well suited for numerical experiments.

The generalization is very simple: instead of the special Hamiltonian equation (4), we can consider more generally a Hamiltonian function $H(x, p_x, z, p_z)$ periodic in $z \in \mathbb{R}$ with period Z, such that for every E in the range under study, the energy surface Σ_E over one period, equation (6), is compact. Then the Floquet treatment of the last section is still valid, and we can still define the number of propagating modes by equation (10). The main results of this paper, equations (26) and (31), can be applied in this general setting.

Note that in the case of electrons in a periodic device, the number of propagating modes could be related to the Landauer conductance at the Fermi energy.

3. The classical dynamics

In order to relate the number of propagating modes $N_{\text{modes}}(E)$, to classical quantities, we introduce here a description of the velocities of the classical trajectories in the wave guide. We note $M = (\vec{x}, \vec{p})$ is a point of phase space, with $\vec{x} \equiv (x, z)$, $\vec{p} \equiv (p_x, p_z)$. The classical equations of motion for $M(t) = (\vec{x}(t), \vec{p}(t))$ corresponding to equation (4) are

$$\partial_t \vec{x} = \partial_{\vec{p}}\mathcal{H} \qquad \partial_t \vec{p} = -\partial_{\vec{x}}\mathcal{H} \tag{16}$$

with

$$\mathcal{H}(\vec{x}, \vec{p}) = \vec{p}^2/2 + V(\vec{x}) \tag{17}$$

being the classical Hamiltonian.

Note that for the Helmholtz equation (1), t is not the true time here, but is linked to the optical length s by $\mathrm{d}s = n|\mathrm{d}\vec{x}| = n^2\mathrm{d}t$, for the special case $E = 0$.

3.1. Ballistic trajectories

It will be shown in the next section that the number of propagating modes $N_{\text{modes}}(E)$ in the semi-classical limit is closely related to the measure of the ballistic trajectories on the energy surface Σ_E. We define them in this section.

The instantaneous z-velocity of a point $M = (\vec{x}, \vec{p})$ of phase space is $v_z = \mathrm{d}z/\mathrm{d}t = \partial_{p_z}\mathcal{H}$. We can then consider the z-velocity from an initial point M averaged over time t by the formula

$$v_t(M) = \frac{1}{t}\int_0^t v_z(M(t'))\,\mathrm{d}t' = \frac{1}{t}\,(z(t) - z(0)) \tag{18}$$

and consider the limit for infinite time, giving the asymptotic velocity

$$v_a(M) = \lim_{t\to\pm\infty} v_t(M). \tag{19}$$

It is a result from the Birkoff ergodic theorem [9] that this limit exists for almost every M and is measurable (because $v_z(M) = \partial_{p_z}\mathcal{H}$ is a Liouville-measurable function on the compact phase space of the cell $z \in [0, Z[$). In the rest of this paper we will call a (positive) ballistic trajectory, a trajectory for which $v_a > 0$.

3.1.1. Distribution of classical velocities. For a given point $M = (\vec{x}, \vec{p})$ of phase space (of the cell $z \in [0, Z[$), we note $E(M) = H(\vec{x}, \vec{p})$ the energy of this point, and $P_t(v_t, E)\mathrm{d}v_t\mathrm{d}E$ the image of the Liouville measure $\nu = \mathrm{d}\vec{x}\mathrm{d}\vec{p}$ on phase space by the application $M \to (v_t(M), E(M))$. In other words, the definition of $P_t(v_t, E)$ is that for any test function $F(v, E)$:

$$\int \mathrm{d}\vec{x}\,\mathrm{d}\vec{p}\,F(v_t, E) = \int F(v_t, E)P_t(v_t, E)\,\mathrm{d}v_t\,\mathrm{d}E. \tag{20}$$

In particular, $P_a(v_a, E) = \lim_{t\to\infty} P_t(v_t, E)$ is the distribution of asymptotic velocities introduced in [1].

3.2. Diffusive trajectories

As a special case, suppose that the dynamics is ergodic on the whole energy surface Σ_E. Then for almost every point $M \in \Sigma_E$, the asymptotic velocity $v_a(M)$ (which is the time average of v_z) is equal to the spatial average of v_z over the energy surface. This spatial average is zero for the Hamiltonian (17), because of the symmetry $p_z \to (-p_z)$. Consequently, the distribution of asymptotic velocities $P_a(v_a, E)$ is a punctual measure at $v_a = 0$.

In the semi-classical limit $\hbar \to 0$, $P_\hbar(v_\hbar, E)$ converges to this punctual measure $P_a(v_a, E) \propto \delta(v_a)$ as shown in [1] (and discussed in the next section, with equation (25)). But this result combined with equation (14) gives a vanishing number of modes. To obtain the leading order expression for $N_{\text{modes}}(E)$, we need to know more precisely in which manner $P_\hbar(v_\hbar, E)$ converges to the punctual measure $P_a(v_a, E)$. We will reach this result in equation (29).

In order to obtain this information we need to make a stronger hypothesis on the dynamics than merely ergodicity: let us suppose that the dynamics on Σ_E is diffusive in the strong sense, which means that if you launch a set of initial conditions $M_i(0)$, then the set of points $M_i(t)$ will diffuse and spread in the guide, and distribute for long times according to a Gaussian distribution with width $\mathcal{D}t$, with $\mathcal{D}$ being the diffusion constant. More precisely, for an initial condition $M \in \Sigma_E$, note $z(t, M)$ is the value of coordinate z after evolution over time t, and $\tilde{z}(t, M) = z(t, M)/\sqrt{t}$ is the rescaled coordinate. The hypothesis of diffusion is that the

image of the measure $\nu = \mathrm{d}\vec{x}\mathrm{d}\vec{p}$ on the phase space, by the application $M \to (\tilde{z}(t, M), E)$ gives for $t \to \infty$, the Gaussian measure,

$$G(\tilde{z}, E)\,\mathrm{d}\tilde{z}\,\mathrm{d}E = \frac{\nu_E}{\sqrt{2\pi\mathcal{D}}}\exp\left(-\frac{\tilde{z}^2}{2\mathcal{D}}\right)\mathrm{d}\tilde{z}\,\mathrm{d}E \tag{21}$$

where

$$\nu_E = \int \delta(E - \mathcal{H}(\vec{x}, \vec{p}))\,\mathrm{d}\vec{x}\,\mathrm{d}\vec{p} \tag{22}$$

is the Liouville measure of the energy surface Σ_E.

By performing the change of variable $v_t = (z(t) - z(0))/t - z(t)/\sqrt{t}$ in equation (21) we obtain that $P_t(v_t, E)$ is a Gaussian distribution which converges towards the punctual measure $P_a(v_a, E) = \nu_E\delta(v_a)$ for $t \to \infty$:

$$P_t(v_t, E) = \frac{\nu_E}{\sqrt{2\pi}}\frac{1}{\sigma_v}\exp\left(-\frac{v_t^2}{2\sigma_v^2}\right) \tag{23}$$

with

$$\sigma_v = \sqrt{\frac{\mathcal{D}}{t}}. \tag{24}$$

Note that, for a given Hamiltonian, it is a difficult problem to check this hypothesis of diffusion and this has been proved rigorously only in very special examples. Heuristically, if the dynamics mixes with positive Lyapunov exponents, the trajectories forget their past after a short time, and almost all of them behave like a Brownian motion, with a diffusive law. In the ergodic regime this hypothesis of diffusion can easily be checked numerically with good accuracy (see section 6.3).

4. Semi-classical correspondence for the distributions of velocities and the number of propagating modes

4.1. Equivalence between the classical and quantum velocity distributions

In [1], Asch and Knauf show the equality of the classical and quantum velocity distributions in the semi-classical limit:

$$P_\hbar(v, E) \equiv P_a(v, E) \qquad \text{for} \quad \hbar \to 0. \tag{25}$$

They proved this for integrable or near-integrable dynamics, with use of quasi-modes, as well for ergodic dynamics (from the Shnirelman theorem). The equality is in the weak sense which means equality with test functions independent of $\hbar$, in other words, equality over intervals of width $\delta v \simeq 1, \delta E \simeq 1$.

As a consequence, from equations (14) (15) and (25), we obtain the leading term for the averaged number of modes equation (15),

$$\langle N_{\text{modes}}(E)\rangle = \frac{1}{h}\mu_{\text{bal}}(E) + o\left(\frac{1}{h}\right) \tag{26}$$

with

$$\mu_{\text{bal}}(E) = \frac{1}{Z}\int_0^{+\infty} v_a P_a(v_a, E)\,\mathrm{d}v_a. \tag{27}$$

So the number of modes $\langle N_{\text{modes}}(E)\rangle$ grows linearly with $1/h$ due to the contribution of the ballistic trajectories. In section 5, we will give a precise geometric interpretation of μ_{bal}, namely as the measure of the ballistic trajectories on a stroboscopic Poincaré section, and equation (26) will look very similar to the Weyl formula.

4.2. A stronger equivalence between the classical and quantum velocity distributions

In the case of an ergodic dynamics, with diffusive behaviour, the asymptotic velocity v_a is zero for almost all trajectories, $P_a(v_a, E) = \nu_E \delta(v_a)$, and we conclude that $\langle N_{\text{modes}}(E)\rangle = o(1/h)$. In order to obtain the leading order of $\langle N_{\text{modes}}(E)\rangle$, we need to know more precisely how the quantum velocity distribution $P_\hbar(v_\hbar, E)$ converges towards $P_a(v_a, E) = \nu_d \delta(v_a)$. For that purpose, we conjecture the following equivalence between the quantum and classical velocity distributions:

$$P_\hbar(v, E) \equiv P_{t_{\text{H}}}(v, E) \qquad \text{for} \quad \hbar \to 0 \tag{28}$$

where t_{H} is the Heisenberg time related to the mean spacing ΔE between energy levels, and to ν_E equation (22), by

$$t_{\text{H}} = \frac{h}{\Delta E} = \frac{\nu_E}{h}.$$

Here the equivalence is supposed to be true over widths $\delta E \sim 1$ and $\delta v \sim \sqrt{h}$ (i.e. with test functions of the form $f(v/\sqrt{h}, E)$).

Then, we obtain from equations (14) and (23),

$$P_\hbar(v_\hbar, E) \equiv \frac{\nu_E}{\sqrt{2\pi}} \frac{1}{\sigma_v} \exp\left(-\frac{v_t^2}{2\sigma_v^2}\right) \qquad \text{for} \quad \hbar \to 0 \tag{29}$$

$$\sigma_v = \sqrt{\frac{\mathcal{D}}{t_{\text{H}}}} = \sqrt{\frac{\mathcal{D}h}{\nu_E}} \tag{30}$$

and

$$\langle N_{\text{modes}}(E)\rangle = \frac{1}{\sqrt{h}} \sqrt{\frac{\nu_E \mathcal{D}}{2\pi Z^2}} + o\left(\frac{1}{\sqrt{h}}\right). \tag{31}$$

So, in the ergodic regime, with diffusive trajectories, (when ballistic trajectories have zero measure), the number of modes $\langle N_{\text{modes}}(E)\rangle$ grows only as the square root of $1/h$. The multiplicative coefficient in front of $1/\sqrt{h}$ involves information from the classical dynamics: the diffusion constant $\mathcal{D}$ and the Liouville measure ν_E of the energy surface.

The conjecture (28) has been justified by different arguments by Eckhardt *et al* in [2]. They relate the variance of a quantum operator $\hat{A}$ to the variance of the integral of the associated classical operator over trajectory segments of length t_{H} (the Heisenberg time). In our case, the operator $\hat{A}$ is the velocity operator $\hat{v}$. They obtain this relation by three different approaches: a semi-classical approach using the contribution of periodic orbits, and two other approaches using random matrix theory and random wavefunction theory.

5. Number of modes from the Poincaré section

In this section we show that the number of modes $N_{\text{modes}}(E)$ expressed in equation (26) is naturally related to properties of the classical Poincaré section of the dynamics: we show that μ_{bal} in formula (26) can be interpreted as the measure of the ballistic trajectories on a stroboscopic Poincaré section.

5.1. Stroboscopic Poincaré section

A convenient way to study the classical dynamics of equation (16) is to follow a trajectory and perform Poincaré sections at periodic values $z = nZ$, $n \in \mathbb{Z}$. In each section, the local canonical coordinates are (x, p_x). This is illustrated in figure 3. In the case of a wave

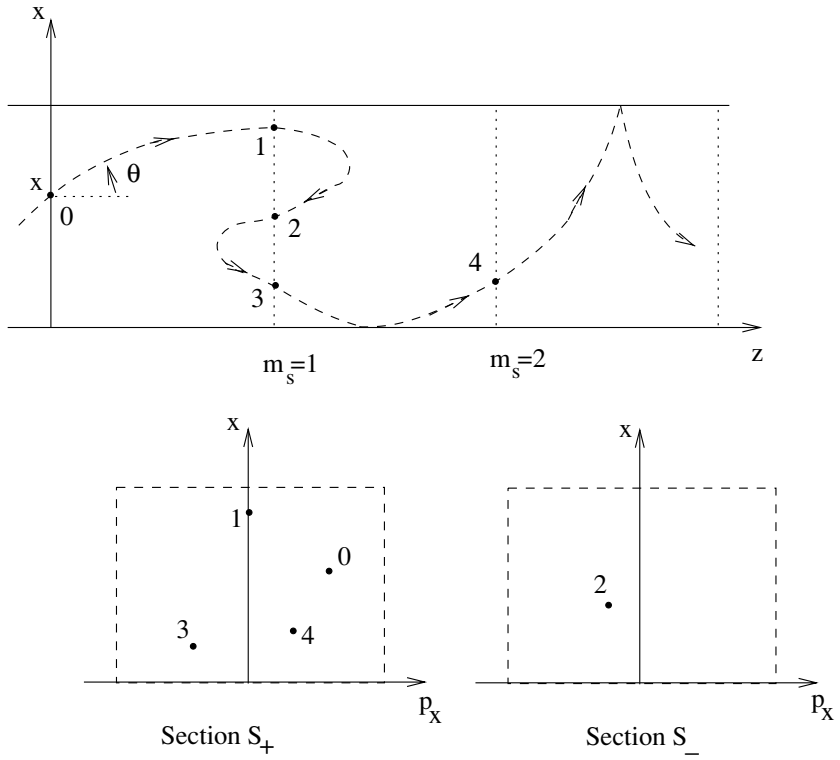

Figure 3. A given trajectory in space (x, z) gives points on the sections S_+ and S_- with coordinates $(x, p_x = n\cos\theta)$. For the last point, $t_s = 4$, $m(t_s) = 2$.

guide, there are two sections to be considered, S_+ and S_-, depending on the sign of p_z at the intersection (see figure 3).

For a given trajectory, with initial point $X = (x, p_x)$ on section S_+ or S_- at $z = 0$, we label the later intersections of the Poincaré sections by $t_s \in \mathbb{Z}$, and the corresponding position $z = mZ$ by

$$m(t_s, X) = z/Z \in \mathbb{Z}. \tag{32}$$

The value of p_x is related to the value of θ at the intersection by $p_x = \mathrm{d}_t x = (\mathrm{d}x/\mathrm{d}\,|\vec{x}|)\,(\mathrm{d}\,|\vec{x}|\,/\mathrm{d}t) = \cos\theta\,.n$.

5.2. Ballistic trajectories

We can consider the Liouville measure ($\mu = \mathrm{d}x\,\mathrm{d}p_x$) of the (positive) ballistic trajectories on the Poincaré sections S^+, S^- by

$$\mu_b = \mu\left(S^+_{\mathrm{bal}}\right) - \mu\left(S^-_{\mathrm{bal}}\right) \qquad S^{\pm}_{\mathrm{bal}} = \{X = (x, p_x) \in S^{\pm} \text{ such that } v_a(X) > 0\}$$

where $v_a(X)$ is defined in equation (19). The difference of measures $\mu\left(S^+_{\mathrm{bal}}\right) - \mu\left(S^-_{\mathrm{bal}}\right)$ is necessary to avoid counting twice a trajectory that would intersect both sections as in figure 3. We will now prove that the measure μ_b defined here is equal to μ_{bal} defined in equation (27).

5.2.1. Example of a uniform guide (continued). We consider again the uniform guide mentioned in section 2.2. In that simple case, every classical trajectory is ballistic, with

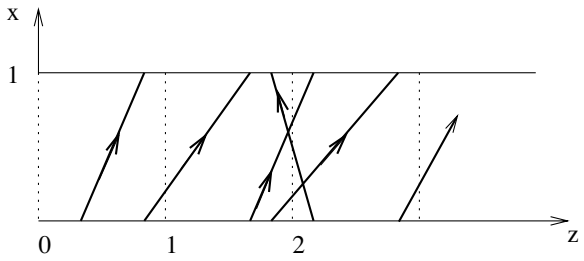

Figure 4. Schematic representation of the trajectories of the kicked Harper Hamiltonian (34) in the guide (z, x). Note the 1-periodicity in x, and the kicking effect at $x = 0$ giving a new direction to the trajectory.

constant velocity v_z. From $p_x = n_0 \cos\theta$, the surface of the Poincaré section is $\mu(S^+) = 2n_0X$, and we deduce that $\mu_b = 2n_0X$. From equation (11) we can write

$$N_{\text{modes}} = \left[\frac{\mu_b}{h}\right]$$

with $h = 2\pi\hbar$. This simple equation is a special case of equation (26) obtained above.

Property.

$$\mu_b(E) = \frac{1}{Z}\int_0^{+\infty} v_a P_a(v_a, E)\,\mathrm{d}v_a. \tag{33}$$

Proof. The left-hand side is a measure on the Poincaré section, while the right-hand side comes from a measure on phase space. We denote $\nu = \mathrm{d}\vec{x}\mathrm{d}\vec{p}$ the measure on phase space, and $\mu = \mathrm{d}x\mathrm{d}p_x$ the measure on the Poincaré sections. Consider U a small set on the Poincaré section S^+, and classical trajectories issued from initial points $M(0)$ in U with energy in $[E, E + \mathrm{d}E[$, followed over time T:

$$V_{T,\mathrm{d}E} = \{M(t) \text{ such that } t \in [0, T], M(0) \in U \times [E, E + \mathrm{d}E[\}\,.$$

For infinitesimal $T = \mathrm{d}t$, we have $\mu(U)\mathrm{d}t\mathrm{d}E = \nu(V_{\mathrm{d}t,\mathrm{d}E})$, just because if $U = \mathrm{d}x\mathrm{d}p_x$, then $\nu(V_{\mathrm{d}t,\,\mathrm{d}E}) = \mathrm{d}x\mathrm{d}p_x\mathrm{d}z\mathrm{d}p_z = \mu(U)\big(\partial_{p_z}\mathcal{H}\big)\mathrm{d}t\mathrm{d}E\big/\big(\partial_{p_z}\mathcal{H}\big) = \mu(U)\mathrm{d}t\mathrm{d}E$. For longer times T this is also true, but the trajectories can again cross the Poincaré sections and have final position $z = mZ = v_T T$. This gives $\nu(V_{T,\mathrm{d}E}) = \mu(U)\frac{mZ}{v_T}\mathrm{d}E$. On the other hand, as can be seen in figure 3, $\mu(U) = \frac{1}{m}\mu_b(U)$. Now by summing over all small sets U, and taking $T \to \infty$, and $v_T \to v_a$, we have: $\mu_b(E') = \int \mathrm{d}E \int_U \mu_b(U)\delta(E-E') = \int \mathrm{d}\vec{x}\,\mathrm{d}\vec{p}\frac{v_a}{Z}\delta(E-E')$. Then applying equation (20) to $F(v, E) = \delta(E - E')v/Z$ gives equation (33). □

6. Results for the kicked Harper model

6.1. The classical kicked Harper model

We now consider one of the simplest models which can illustrate the results of this paper. The dynamics takes place in a two-dimensional guide (z, x), infinite and 1-periodic in z and confined in x (we identify $x = 1$ with $x = 0$). The classical trajectories are straight lines in the positive x-direction with constant x-velocity. When a trajectory reaches the boundary $x = 1$, it is re-injected at $x = 0$ with the same z-value, but with a different direction, which depends periodically on z (this mimics a periodic billiard) (see figure 4).

Such a dynamics can be generated by the following Hamiltonian:

$$H(x, p_x, z, p_z) = p_x + H_1(p_z) + H_2(z)\delta(x) \tag{34}$$

with

$$H_1(p_z) = -\frac{\gamma}{2\pi}\cos(2\pi p_z) \tag{35}$$

$$H_2(z) = -\frac{\gamma}{10\pi}\cos(2\pi z). \tag{36}$$

H is indeed periodic in z with period $Z = 1$.

The phase space is spanned by the four variables: $x \in [0, 1[\equiv \mathbb{R}/\mathbb{Z}$, $p_x \in \mathbb{R}$, $z \in \mathbb{R}$, $p_z \in [0, 1[\equiv \mathbb{R}/\mathbb{Z}$. The periodicity in p_z has been chosen by simplicity, so that $p_z \in [0, 1[$.

The parameter $\gamma \in \mathbb{R}$ is fixed and determines the nature of the dynamics.

For a fixed total energy E and for the first two variables, the classical equations of motion are

$$\frac{\mathrm{d}x}{\mathrm{d}t} = 1 \qquad \frac{\mathrm{d}p_x}{\mathrm{d}t} = 0$$

so $x \equiv t$ *modulo* 1 (by a suitable choice of time origin: $x(0) = 0$), and for the last two variables:

$$\frac{\mathrm{d}z}{\mathrm{d}t} = \frac{\partial H_1}{\partial p_z} \tag{37}$$

$$\frac{\mathrm{d}p_z}{\mathrm{d}t} = -\frac{\partial H_2}{\partial z}\sum_{k\in\mathbb{Z}}\delta(t-k). \tag{38}$$

These last two equations define the usual kicked Harper model [10], with a one degree of freedom, time-dependent Hamiltonian:

$$H_{\mathrm{KH}}(z, p_z, t) = H_1(p_z) + H_2(z)\sum_{k\in\mathbb{Z}}\delta(t-k). \tag{39}$$

The trick in equation (34), which is time independent, was to use the periodic x variable as the effective time t.

Equation (37) can be integrated over a period $t = 0^+ \to 1^+$ and give the Poincaré mapping corresponding to successive intersections of a trajectory with the boundary $x = 0^+$:

$$\begin{cases} z' = z + \gamma\sin(2\pi p_z) \\ p_z' = p_z - \frac{\gamma}{5}\sin(2\pi z'). \end{cases} \tag{40}$$

The Poincaré sections of the trajectories give an idea of the regularity or chaotic behaviour of the dynamics. Figure 5 shows the Poincaré sections, where the values of z *modulo* 1 values have been plotted in the interval $[0, 1[$. For $\gamma \to 0$, the dynamics is nearly integrable, for $\gamma = 0.5$ the phase space is mixed, with regular part and chaotic zones, while for $\gamma = 1.2$ the dynamics seems to be ergodic and strongly chaotic on the whole energy surface. For $\gamma = 0.2$–0.5, we clearly see regular ballistic trajectories (for the z-direction), near $p_z \simeq 0.3, 0.7$. There remains a very narrow ballistic component at $\gamma = 0.7$ which separates two chaotic regions, and the ballistic trajectories disappear for $\gamma > 0.7$. For $\gamma = 1.2$, the whole phase space is occupied by a single chaotic component.

From this Poincaré mapping, it is easy to study numerically the evolution of a trajectory issued from an initial condition (z_0, p_{z0}). We consider the natural measure $\mathrm{d}z\mathrm{d}p_z$ on this Poincaré section, and its image by the application of $z \to v_t = z(t)/t$. This gives the distribution of classical velocities $P_z(v_t)\mathrm{d}v_t$ which can easily be calculated numerically

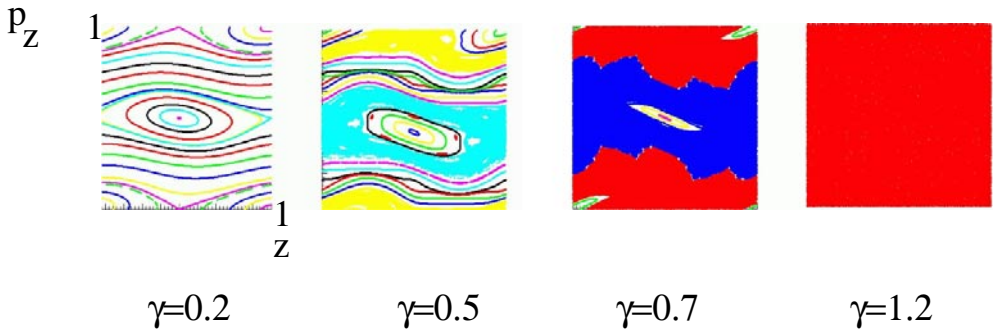

Figure 5. Poincaré section of the trajectories obtained by the mapping (40) for different values of the dynamical parameter γ.

(This figure is in colour only in the electronic version)

(by discretizing the Poincaré section). Due to the simple dependence on p_x in equation (34), this distribution is in fact identical to the distribution $P(v_t, E)$ defined in section 3.1:

Property.

$$P_t(v_t, E) = P_z(v_t) \qquad \forall E \qquad \text{for} \quad t \to \infty.$$

Proof. We have $\mathrm{d}\vec{x}\,\mathrm{d}\vec{p} = \mathrm{d}z\mathrm{d}p_z\mathrm{d}x\mathrm{d}p_x = (\mathrm{d}z\mathrm{d}p_z)\big(\partial_{p_x}\mathcal{H}\big)\,\mathrm{d}t\mathrm{d}E\big/\big(\partial_{p_x}\mathcal{H}\big) = (\mathrm{d}z\mathrm{d}p_z)\mathrm{d}t\mathrm{d}E$. So for any function $F(v, E)$ we have on the one hand equation (20), and on the other (because $\mathrm{d}t = \mathrm{d}x$) $\int \mathrm{d}\vec{x}\,\mathrm{d}\vec{p}\,F(v_t, E) = \int \mathrm{d}x\,\mathrm{d}E\,\mathrm{d}z\,\mathrm{d}p_z F(v_t, E) = \int \mathrm{d}v_t\,\mathrm{d}E\,F(v_t, E)P_z(v_t)$, giving the result. □

6.2. The quantum kicked Harper model

After quantization, the Hilbert space, consists of wavefunctions $\phi(x, z)$ periodic in x modulo a fixed phase φ, and with a Fourier transform $\hat{\phi}(p_x, p_z)$ periodic in p_z modulo a given phase θ_2,

$$\phi(x + 1, z) = \mathrm{e}^{\mathrm{i}\varphi}\phi(x, z) \tag{41}$$

$$\hat{\phi}(p_x, p_z + 1) = \mathrm{e}^{-\mathrm{i}\theta_2}\hat{\phi}(p_x, p_z). \tag{42}$$

So the quantization procedure depends on the choice of these two phases (φ, θ_2) in $[0, 2\pi[^2$.

Because of the periodicity of H in z, we work with the Floquet condition (5) giving

$$\phi(x, z + 1) = \mathrm{e}^{\mathrm{i}\theta}\phi(x, z). \tag{43}$$

The stationary equation (3) here gives

$$\hat{H}\phi = E\phi \qquad \mathrm{i}\hbar\partial_x\phi(x, z) = \hat{H}_{\mathrm{KH}}(x)\phi(x, z) - E\phi(x, z).$$

(Here E is fixed, $\hat{H}_{\mathrm{KH}}(t)$ is the quantization of equation (39), and x can be replaced by t). This x-dependent Schrödinger equation can be integrated over a period $x = 0^+ \to 1^+$, giving a unitary propagator $\hat{U} = \exp(-\mathrm{i}H_2/\hbar)\exp(-\mathrm{i}H_2/\hbar)$, and

$$\phi(x + 1, z) = \mathrm{e}^{\mathrm{i}E/\hbar}\hat{U}\phi(x, z) = \mathrm{e}^{\mathrm{i}\varphi}\phi(x, z). \tag{44}$$

The solutions ϕ of this equation are then the eigenvectors of the unitary propagator $\hat{U}$ with eigenvalues $\varphi_n \in [0, 2\pi[$:

$$\hat{U}\phi_n = \mathrm{e}^{\mathrm{i}\varphi_n}\phi_n \tag{45}$$

$$\frac{E}{\hbar} + \varphi_n \equiv \varphi[2\pi]. \tag{46}$$

The observation is that the propagating modes at energy $E = 0$ we are looking for are just the solutions of equation (44), i.e. the so-called 'quasi-stationary' states of the kicked Harper model for a fixed quasi-energy φ. If all the quasi-energies $\varphi_n(\theta)$ are calculated, the propagating modes are obtained by intersections of this spectrum at fixed φ, as in figure 9(a).

After a few calculations, we obtain that the quantum velocity defined in equation (12) is equal to the derivatives of the quasi-energies:

$$v_\hbar = \langle \phi_n(\theta) | \hat{v}_z | \phi_n(\theta) \rangle = \frac{\mathrm{d}\varphi_n}{\mathrm{d}\theta}. \tag{47}$$

From equation (46), we see that the number of modes $\langle N_{\mathrm{modes}}(E) \rangle$ averaged over an interval of energy of width $\delta E \simeq h$ is equal to the number of modes $N_{\mathrm{modes}}(\varphi)$ averaged over the width $\delta\varphi \simeq 2\pi$:

$$\langle N_{\mathrm{modes}} \rangle_\varphi = \frac{1}{2\pi} \int_0^{2\pi} N_{\mathrm{modes}}(\varphi).$$

So in practice (i.e. with numerical computation) we calculate the whole spectrum $\varphi_n(\theta)$ for $n = 1 \to N$ and $\theta \in [0, 2\pi[$, as in figure 9(a). The distributions of slope $\mathrm{d}\varphi_n/\mathrm{d}\theta$ are then easily measured, giving the distribution of quantum velocities $P_\hbar(v_\hbar)$, and finally $\langle N_{\mathrm{modes}} \rangle_\varphi$ with the use of equation (14).

6.2.1. Remark on quantization. Because of the non-commutativity of operators $\hat{z}$ and $\hat{p}_z$, it is well known that at fixed x, the periodicity conditions (41) and (43) in z, p_z for a function $\phi(x, z)$ can be realized only if $\hbar$ fulfils the integral condition [6]:

$$N = \frac{1}{2\pi\hbar} \in \mathbb{N}.$$

The Hilbert space of functions $\phi(x, z)$ (at fixed x) is then a space $\mathcal{H}_N(\theta, \theta_2)$ of finite dimension $N = 1/h$, and $N \to \infty$ is the semi-classical limit.

6.3. Numerical results

6.3.1. In the nearly integrable regime. We see in the Poincaré section of figure 5, that for $\gamma = 0.2$ the dynamics is nearly integrable. It is also clearly visible that there are two kinds of trajectories. The first kind of trajectories which give the two elliptical family sets in the Poincaré sections is confined because $z(t)$ is bounded. The second kind of trajectories which give horizontal curves in figure 5 is ballistic.

Figure 6 shows the distribution of classical velocities $P_t(v_t)$ for $t = 10, 100, 1000$. For large t the distribution converges towards the distribution of asymptotic velocities $P_a(v_a)$, where the ballistic trajectories contribute for $v_a \neq 0$, and the confined trajectories are responsible for the central peak. Note that this central peak converges towards a Dirac distribution with width $\delta_t \simeq 1/t$.

In the quantum spectrum the two sets of trajectories are also visible, see figure 7(a), giving two different sets of bands: bands with non-zero slopes (from quantum states localized on ballistic trajectories) and bands with zero slope (from quantum states localized on confined trajectories). The distribution of quantum velocities obtained from this quantum spectrum is very close to the classical distribution as predicted from equation (25).

With this regular dynamics, with ballistic trajectories, the number of modes $\langle N_{\mathrm{modes}} \rangle$ is a linear function of $1/h$ as stated by equation (26).

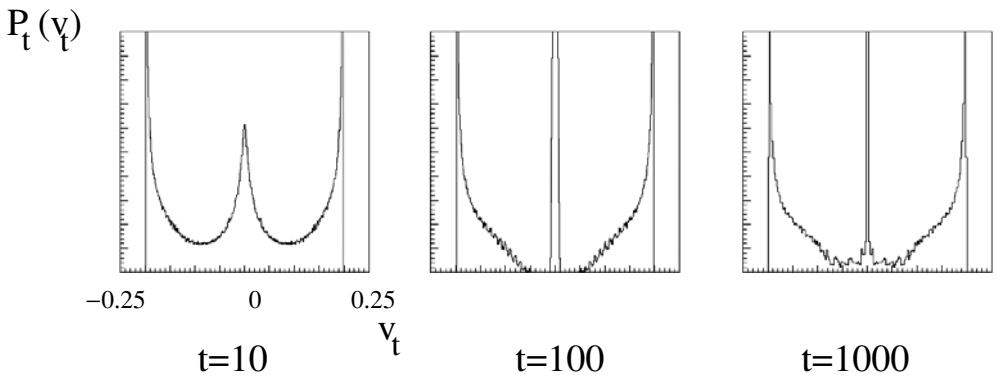

Figure 6. Distribution of classical velocities $P_t(v_t)$ for $\gamma = 0.2$ and $t = 10$, 100, 1000. The distribution reflects the two sets of trajectories: the ballistic trajectories with non-zero asymptotic velocities, and the confined trajectories which give the central peak.

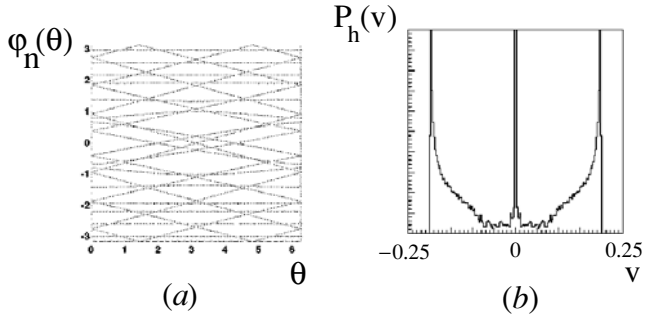

Figure 7. (*a*) The band spectrum $\varphi_n(\theta)$, for a regular dynamics ($\gamma = 0.2$), for $1/h = 30$. (*b*) The distribution of quantum velocities $P_\hbar(v_\hbar)$ obtained from the spectrum for $1/h = 500$. The distribution is very similar to the classical distribution of asymptotic velocities (see figure 6, with $t = 1000$), as predicted by equation (25).

6.3.2. In the ergodic regime. From the Poincaré section, figure 5, for $\gamma = 1.2$ the dynamics seems to be ergodic on phase space. We compute the distribution of the classical velocities $P_t(v_t, E)$ for $t = 200, 10^3, 10^4, 10^5$ (see figure 8). The distribution is well fitted to the Gaussian model of diffusion equation (23). This fit gives the following values for the diffusion constant $\mathcal{D}$:

t	200	10^3	10^4	10^5
$\mathcal{D}$	2.54	2.56	2.58	2.58

The nearly stable value of $\mathcal{D}$ for large t confirms the diffusion property of the dynamics.

We now consider the corresponding quantum model. Figure 9(*a*) shows a part of the spectrum (46) $\varphi_n(\theta)$ calculated numerically for $1/h = 200$. We observe that the energy curves undulate with clearly visible avoided crossings. The distribution of slopes $\mathrm{d}\varphi_n/\mathrm{d}\theta$ measured on this spectrum gives us directly with equation (47) the distribution of quantum velocities $P_\hbar(v_\hbar)$, shown in figure 9(*b*). This distribution is well fitted by the expected Gaussian law equation (29).

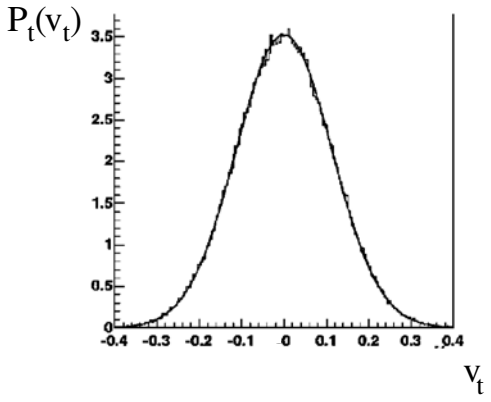

Figure 8. Distribution of classical velocities $P_t(v_t)$ for $t = 200$, and a completely ergodic and diffusive dynamics ($\gamma = 1.2$). The distribution is well fitted by a Gaussian giving a diffusion constant $\mathcal{D} \simeq 2.54$.

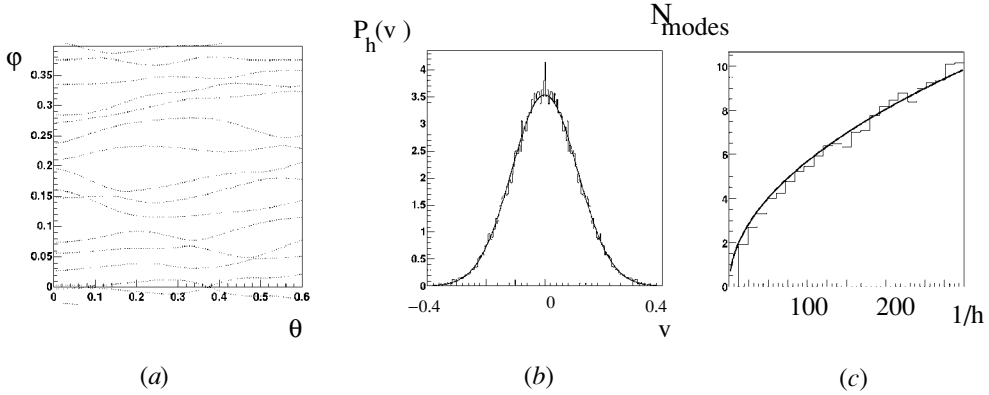

Figure 9. (a) A part of the band spectrum $\varphi_n(\theta)$, for ergodic and diffusive dynamics ($\gamma = 1.2$), for $1/h = 200$. (b) Distribution of quantum velocities $P_\hbar(v_\hbar)$ obtained from this spectrum. The distribution is well fitted by the expected Gaussian equation (29) giving a constant $\mathcal{D}_q \simeq 2.52$, in very good agreement with the classical diffusion constant. (c) The average number of modes $\langle N_{\text{modes}} \rangle$ in the wave guide as a function of $1/h$ is well fitted by the expected curve $\frac{1}{\sqrt{h}}\sqrt{\frac{\mathcal{D}}{2\pi}}$, with $\mathcal{D} = 2.54$.

The fit gives an effective constant $\mathcal{D}_q \simeq 2.52$ which is in very good agreement with the classical measure of the diffusion constant of figure 8.

Finally, the average number of propagating modes $\langle N_{\text{modes}} \rangle$ is directly obtained from the quantum velocities distribution by equation (14). Figure 9(c) shows $\langle N_{\text{modes}} \rangle$ as a function of $1/h$ and a fit with the expected result (31), which reads in the kicked Harper model ($\nu_E = 1, Z = 1$)

$$\langle N_{\text{modes}}(E) \rangle = \frac{1}{\sqrt{h}}\sqrt{\frac{\mathcal{D}}{2\pi}} + o\left(\frac{1}{\sqrt{h}}\right).$$

The fit with a constant $\mathcal{D} = 2.52$, is again in very good agreement with the classical measure of the diffusion constant.

7. Conclusion

We have given precise expressions (26) and (31) for the number of propagating modes N_{modes} in a periodic wave guide in terms of the classical transport quantities, such as the measure of ballistic trajectories or the diffusion constant. These results are obtained in the semi-classical limit and have been confirmed by numerical calculations.

Concerning the relevance of our results to concrete physical problems, we have to discuss the limitations of our idealized model, due to unavoidable effects such as absorption or low disorder. We will stay on a qualitative level of discussion.

The main parameter which characterizes the absorption effects is the absorption length l_{abs}. For a ballistic wave, this length is related to the time τ_{abs} after which the wave is significantly attenuated by the equation $l_{\text{abs}} = \langle v \rangle \tau_{\text{abs}}$, where $\langle v \rangle$ is the group velocity. These effects perturb the spectrum and give a finite width to the energy levels, on a scale $\Delta E_{\text{abs}} \simeq \hbar/\tau_{\text{abs}}$. Our results, in particular the measure of N_{modes}, will not be affected by these absorption effects, as long as ΔE_{abs} is much less than the mean spacing between energy levels ΔE introduced in section 4.2. Similarly, for a guide with a finite total length L, there are corrections of order $\Delta E_L \simeq \hbar \langle v \rangle / L$, which do not affect our results if $\Delta E_L \ll \Delta E$. This is possible if L is large enough (see [13] for a precise analysis). The same observation can be made for the effects of a low disorder in the guide, which, in principle, induces localization, characterized by a localization length l_{loc} and a pure point spectrum. They can also be neglected if $l_{\text{loc}} \gg L$.

The conductance N_{modes} in periodic structures is very accessible experimentally. The different and non-trivial manifestations of classical transport properties on the wave conductance shown in this paper can be observed in various domains of physics: in acoustics with sound waves in water, or in quantum waves physics with cold atoms or electrons in mesoscopic devices [13], and finally with optical waves [11]. At the same time they concern still open problems in mathematics [1].

This study can be pursued and completed by considering different problems we have not discussed here. In the case of mixed classical dynamics, with chaos and regular stable islands, in the frontier between ballistic and diffusive trajectories, anomalous diffusion of the Lévy type can occur [7]. It would be interesting to know how such anomalous transport manifests itself in the value of N_{modes}. Another interesting effect is for an ergodic and diffusive guide, if the localization process takes place before quantum ergodicity is reached (i.e. if the break time is less than the Heisenberg time), in the same manner it occurs in rough billiards [4]. These phenomena can occur in an intermediate regime in the semi-classical limit $h \to 0$. The effect is then an enhancement of the conductance N_{modes}, already mentioned by Shepelianskii [10].

In this paper we have treated the case of a two-dimensional guide (x, z) periodic in the z-direction. Our results can be extended easily for more dimensions. For three dimensions, formulae (26) and (31) become $\langle N_{\text{modes}}(E) \rangle \propto 1/h^2$ and $\langle N_{\text{modes}}(E) \rangle \propto 1/h$ respectively.

Acknowledgment

The author gratefully acknowledges Christian Miniaturat for stimulating discussions.

References

[1] Asch J and Knauf A 1998 Motion in periodic potentials *Nonlinearity* **11** 175–200

[2] Eckhardt B, Fishman S, Keating J, Agam O, Main J and Müller K 1995 Approach to ergodicity in quantum wave functions *Phys. Rev.* E **52** 5893–903

[3] Pichard J-L 1994 *Mesoscopic Quantum Physics*. *Proc*. *Les Houches Summer School, Session LXI* ed E Akkermans and G Montambaux
[4] Frahm K M and Shepelyansky D L 1997 Quantum localization in rough billiards *Phys*. *Rev. Lett*. **78** 1440–3
[5] Gutzwiller M 1991 *Chaos in Classical and Quantum Mechanics* (New York: Springer)
[6] Lebœuf P, Kurchan J, Feingold M and Arovas D P 1990 Phase-space localization: topological aspects of quantum chaos *Phys*. *Rev. Lett*. **65** 3076–9
[7] Leboeuf P 1998 Normal and anomalous diffusion in a deterministic area-preserving map *Physica* D **116** 8–20
[8] Zengerle R 1987 Light propagation in singly and doubly periodic planar waveguides *J*. *Mod*. *Opt*. **34** 1589–617
[9] Reed M and Simon B 1978 *Mathematical Methods in Physics vol I: Functional Analysis* (New York: Academic)
[10] Shepelyansky D and Lima R 1991 Fast delocalization in a model of quantum kicked rotator *Phys*. *Rev. Lett*. **67** 1377–80
[11] Gonçalves R R, Ribeiro S J L and Messaddeq Y 2000 Low optical loss planar waveguides prepared in an organic–inorganic hybrid system *Appl*. *Phys*. *Lett*. **77** 3502–4
[12] Pagneux V 1996 Propagation acoustique dans les guides à section variable et effets d'écoulement *Thèse de doctorat* Université du Maine, France
[13] Liang W, Bockrath M, Bozovic D, Hafner J H, Tinkham M and Park H 2001 Fabry–Perot interference in a nanotube electron waveguide *Nature* **411** 665–9